HHS Public Access

Author manuscript

J Magn Reson Imaging. Author manuscript; available in PMC 2020 June 01.

Published in final edited form as:

J Magn Reson Imaging. 2019 June ; 49(7): e195–e204. doi:10.1002/jmri.26600.

Targeted Rapid Knee MRI Exam using T2 Shuffling

Jonathan I. Tamir, PhD[1], **Valentina Taviani, PhD**[2], **Marcus T. Alley, PhD**[3], **Becki Perkins, RT**[4], **Lori Hart**[4], **Kendall Obrien, BA**[4], **Fidaa Wishah, MD**[3], **Jesse K Sandberg, MD**[3], **Michael J. Anderson, PhD**[5], **Javier S. Turek, PhD**[6], **Theodore L. Willke, PhD**[6], **Michael Lustig, PhD**[1], and **Shreyas S. Vasanawala, MD, PhD**[3]

[1]Department of Electrical Engineering and Computer Sciences, University of California, Berkeley, California, USA

[2]Global Applied Science Laboratory, GE Healthcare, Menlo Park, California, USA

[3]Department of Radiology, Stanford University, Stanford, California, USA

[4]Department of Radiology, Lucile Packard Children's Hospital, Stanford, California, USA

[5]Parallel Computing Lab, Intel Labs, Santa Clara, California, USA

[6]Brain-Inspired Computing Lab, Intel Labs, Hillsboro, Oregon, USA

Abstract

Background: MRI is commonly used to evaluate pediatric musculoskeletal pathologies, but same-day/near-term scheduling and short exams remain challenges.

Purpose: To investigate the feasibility of a targeted rapid pediatric knee MRI exam, with the goal of reducing cost and enabling same-day MRI access.

Study Type: Cost effectiveness study done prospectively.

Subjects: 47 pediatric patients.

Field Strength/sequence : 3T. The 10-minute protocol was based on T2 Shuffling, a four-dimensional acquisition and reconstruction of images with variable T2 contrast, and a T1 2D FSE sequence. A distributed, compressed sensing-based reconstruction was implemented on a four-node high-performance compute cluster and integrated into the clinical workflow.

Assessment: In an institutional review board approved study with informed consent/assent, we implemented a targeted pediatric knee MRI exam for assessing pediatric knee pain. Pediatric patients were sub-selected for the exam based on insurance plan and clinical indication. Over a two-year period, 47 subjects were recruited for the study and 49 MRIs were ordered. Date and time information was recorded for MRI referral, registration, and completion. Image quality was assessed from 0 (non-diagnostic) to 5 (outstanding) by two readers, and consensus was subsequently reached.

Corresponding Author Information: Jonathan I. Tamir, 468 Cory Hall, Department of Electrical Engineering and Computer Sciences, University of California, Berkeley, Berkeley, CA 94720, jtamir@eecs.berkeley.edu.

Statistical Tests: A Wilcoxon rank-sum test assessed the null hypothesis that the targeted exam times compared to conventional knee exam times were unchanged.

Results: Of the 49 cases, 20 were completed on the same day as exam referral. Median time from registration to exam completion was 18.7 minutes. Median reconstruction time for T2 Shuffling was reduced from 18.9 minutes to 95 seconds using the distributed implementation. Technical fees charged for the targeted exam were one third that of the routine clinical knee exam. No subject had to return for additional imaging.

Data Conclusion: The targeted knee MRI exam is feasible and reduces the imaging time, cost, and barrier to same-day MRI access for pediatric patients.

Keywords

MR value; T2 Shuffling; 3D FSE; Turbo spin-echo (TSE); Compressed sensing; Rapid multi-contrast imaging

INTRODUCTION

Magnetic resonance imaging (MRI) is a common diagnostic method for evaluating various musculoskeletal pathologies. In children and adolescents, the knee is the most common joint assessed with MRI (1). Between 2011 and 2014, approximately 5.6 million sports and recreation related injuries occurred in child and adolescent populations, accounting for 28% of emergency visits (2). Among these visits, 42% were due to lower extremity injuries (3).

In very young pediatric patients, knee MRI is often used to evaluate developmental conditions and non-traumatic pain (4). In pediatric populations, common injuries are meniscal pathology, cruciate ligament tears, and cartilage abnormalities; these are assessed well with MRI (1). Despite its advantages, MRI of the pediatric knee presents several challenges due to requirements for high (sub-millimeter) spatial resolution, leading to lengthy scan and exam times. As a result, increased patient anxiety and discomfort may lead to motion, resulting in imaging artifacts. A secondary effect of the long exams is high cost, limiting the value of the MRI exam in the context of clinical care.

Typically, patients first access care through a consultation visit with an orthopedic surgeon. Based on the clinical indication, the orthopedist may request an MRI. After insurance authorization is granted, the patient is scheduled for an MRI, usually in the following weeks. The scheduling process is often long, and the appointment is usually disruptive to work for parents and to school for children. Following insurance authorization and exam scheduling, the patient returns on the scheduled date for the MRI. The MRI protocol for routine knee imaging often consists of multiple two-dimensional (2D) fast spin-echo (FSE) acquisitions, each at a different orientation to account for voxel anisotropy, as well as at a different target image contrasts to assess various pathology (5, 6). For pediatric patients, the exam typically lasts between 25 to 45 minutes.

Volumetric alternatives to the standard knee protocol are attractive because they theoretically provide isotropic resolution and larger slice coverage, enabling multiplanar reformats and eliminating the need to separately scan at multiple orientations with additional technologist

planning. The primary challenge with 3D FSE acquisitions is the tradeoff between scan time and image blurring due to long echo trains (7). Parallel imaging (8, 9) and compressed sensing (10) combined with variable refocusing flip angles (7, 11) have been used to accelerate 3D FSE knee imaging to obtain whole coverage in 5 minutes (12–14). Nonetheless, true clinical adoption with replacement of conventional 2D imaging is seldom described, likely due to persistent blurring artifacts. In recent work, a fast pediatric knee exam consisting of two 5-minute 3D FSE scans has demonstrated excellent sensitivity and specificity compared to arthroscopy (15). A double-echo steady state (DESS) sequence was also proposed for 3D coverage in 5 minutes, simultaneously providing morphology and quantitative T2 values with near-isotropic resolution (16). The approach shows excellent sensitivity and specificity for evaluating osteoarthritis pathology, but the unfamiliar image contrasts produced by DESS require further evaluation for clinical adoption, particularly for a pediatric setting.

An acquisition based on 3D FSE was recently proposed that permits volumetric reconstruction of images with contrast varying from proton-density (PD) weighting to increasing T2 weighting (17). This seven-minute acquisition, termed T2 Shuffling (T2Sh), uses ideas from compressed sensing to accelerate the acquisition and mitigate blurring due to T2 decay by accounting for relaxation behavior. A prior study with 30 consecutive patients investigating a single-sequence protocol using T2Sh, compared against the conventional protocol, indicated that missing clinically relevant pathology is unlikely (18). The use of T2Sh in a targeted exam is attractive as it provides isotropic-resolution images at multiple clinical contrasts, obviating the need for a number of conventional 2D scans. The purpose of this study was to determine feasibility and impact of a targeted rapid MRI exam based on T2Sh for pediatric knee imaging at 3T.

MATERIALS AND METHODS

Patient Recruitment:

With institutional review board approval and informed patient consent and/or assent, a targeted knee MRI exam for evaluating pediatric knee pain was implemented in our institution on two 3T MRI scanners (MR750, GE Healthcare, Waukesha, WI USA) with 16 channel flex coil arrays (GEM Suite, GE Healthcare, Waukesha, WI USA). Insurance plans were reviewed to sub-select those plans with high likelihood of waived authorization, rapid authorization, or retroactive insurance authorization. Patients with indications of anterior knee pain, suspicion of osteochondral lesions, anterior cruciate ligament (ACL) tears, and meniscal pathology were eligible for the rapid protocol knee MRI exam, given that prior work validated the accuracy of diagnosing these conditions (18). A mechanism of communication between the orthopedic surgical clinic and an adjacent MRI scanner (10 meters from the clinic) was established. When a targeted knee MRI was requested, a Current Protocol Terminology (CPT) 52 modifier code was included to indicate a reduced charge relative to the routine lower extremity joint without contrast (CPT 73721). From October 2016 to May 2018, 47 subjects (mean age 14, 19 male, 28 female) satisfying the inclusion criteria were recruited. Two patients had requests for bilateral knee MRIs, resulting in 49 targeted knee MRI orders. Patients were accommodated into the clinical schedule by

leveraging two detachable MRI tables such that a patient could be prepared and placed on one table while the prior patient was still getting scanned on the other.

Data Acquisition:

A four-dimensional FSE acquisition, termed T2Sh, that encodes the knee anatomy in a volumetric fashion and also permits reconstruction of images with variable T2 contrast, was implemented (17). The acquisition used a randomized view ordering to re-acquire phase encode samples during the FSE echo trains. A 10-minute targeted knee MRI protocol was designed, consisting of a localizer (1 minute), fat-suppressed (FS) T2Sh (7 minutes) with source images reconstructed in the sagittal plane, and a 2D coronal non-FS FSE T1 (3 minutes).

Based on technologist evaluation, scans were repeated or added if necessary, e.g. due to motion artifacts or incorrectly prescribed field of view (FOV). The typical prescribed scan parameters, shown in Table 1, were modified from those reported in a previous clinical study (18). The repetition time (TR) for the T2Sh scan was lowered from 1400 ms to 1200 ms to increase scan efficiency, as the increased T1 weighting was found to be tolerable. In addition, a partial Fourier fraction of 65% was used as it was found to reduce residual incoherent artifacts (19). Scan parameters (e.g. FOV, number of slices) were adjusted slightly for each patient on a case-by-case basis, as part of routine clinical practice.

Image Reconstruction:

The T2Sh reconstruction was initially implemented as described in (17, 18, 20), and reconstruction parameters were held fixed during the study. Coil compression to seven virtual channels was used to accelerate the reconstruction (21). To improve robustness to FOV prescription, two sets of Soft-SENSE coil sensitivity maps were estimated using ESPIRiT (22), an auto-calibrating parallel imaging method. ESPIRiT parameters were selected using a parameter-free approach based on a noise pre-scan (23). Each slice was reconstructed independently following a Fourier transform in the readout direction. Four basis coefficient images were used in the T2Sh reconstruction, and locally low rank regularization was used with a 12-by-12 patch size and regularization value of 0.0125 (17). The FISTA iterative algorithm was used with 250 iterations (24). End-to-end processing, i.e. raw data to final DICOM images, was integrated into the hospital environment so that the images could be auto-transferred to the scanner console and to the Picture and Archiving Communication System (PACS) following reconstruction.

Using the Orchestra software development kit (GE Healthcare, Waukesha, WI USA), the raw data were converted to a data format compatible with the Berkeley Advanced Reconstruction Toolbox (BART) (25, 26). The reconstruction, including coil compression, coil sensitivity calibration, iterative compressed sensing, and Homodyne filtering (27), were carried out with BART. Following the reconstruction, gradient non-linearity correction was applied, and the results were saved as DICOM images using Orchestra.

Ongoing work during the study led to an efficient, distributed implementation of the reconstruction that leveraged multiple machines with multiple computer processing units (20). A four-node high performance computing cluster was deployed at the hospital in

January, 2018 and connected to a local network shared by the scanner and the hospital PACS through a one-gigabit-per-second (Gbps) connection. The compute cluster had an internal 10 Gbps network. Each compute node had a dual-socket Intel® Xeon®[1] Platinum 8180 processor with 28 cores and 192 GB of RAM (Intel Corporation, Santa Clara, CA, USA). Reconstructed sagittal source images corresponding to contrast-equivalent echo times (TE) (11) of 20 ms (PD weighted), 50 ms (intermediate weighted), and 100 ms (T2 weighted) were sent to the scanner and to the PACS. Following the reconstruction, images were reformatted by the technologist on the scanner console into axial, sagittal, and coronal planes with 2.4 mm slice thickness and 50% overlap between slices.

Evaluation:

Date and time information was recorded for MRI exam referral and registration. Start and end times were logged for each sequence in the exam and used to assess total exam times. Descriptive statistics related to the patient cohort and the scans were analyzed, including instances where scans were repeated. Clinical indications leading to the MRI order were also noted. End-to-end reconstruction times were evaluated before and after the deployment of the distributed cluster. Image quality was assessed by two readers (J.S. and F.W., 4 and 8 years' experience respectively) on a scale from 0 (non-diagnostic) to 5 (outstanding anatomy delineation), and consensus was subsequently reached.

To determine the impact on access to MRI and ability to offer walk-in scans, the MRI scheduling times were also compared to those of a control cohort of 50 consecutive patients referred for the conventional lower extremity knee MRI. The conventional exam consisted of the following 2D sequences: axial PD FS, coronal T2 FS, coronal T1, sagittal PD FS, sagittal PD, and sagittal T2 FS. A one-sided Wilcoxon rank sum test assessed the null hypothesis that the scheduling time between MRI order and exam dates for the targeted and conventional exams is unchanged. Additionally, targeted MRI exam times were also compared to those of the conventional knee MRI exam across 20 consecutive patients before the introduction of T2Sh. Another one-sided Wilcoxin rank sum test assessed the null hypothesis that exam times for the targeted and conventional exams were unchanged. Patients were not scanned with both the targeted protocol and the conventional protocol.

RESULTS

Figure 1 shows a bar chart of the primary clinical indication for each exam order, as well as image quality consensus ratings. The most common reason for exam referral was to evaluate meniscal tear, followed by knee pain. Greater than 85% of the cases were rated as very good to outstanding. No exams were deemed non-diagnostic or poor quality. Due to the inclusion of a CPT modifier code, the technical fees of the targeted knee MRI were reduced to one third the cost of the routine knee MRI.

Figure 2 shows two representative cases referred for meniscal tear. The first case shows T2Sh images reformatted into PD weighted sagittal, T2 weighted coronal, and intermediate

[1]Intel and Xeon are trademarks of Intel Corporation or its subsidiaries in the U.S. and/or other countries. Other names and brands may be claimed as the property of others.

weighted axial planes. Note the sharpness of the reformatted images, which confirmed a meniscal tear. In the second case, the clinical suspicion was a meniscal tear, but the MRI diagnosis was a bone bruise. The edema in the bone is well-visualized in the coronal T2 weighted reformat of the T2Sh images and also seen in the T1 coronal image.

Figure 3 shows the MRI findings for a 15-year-old male patient evaluated for ACL and meniscal tears. The T2Sh image reformatted into sagittal PD weighting shows increased signal with indistinct ACL fibers consistent with high grade tear. The T1 coronal image shows a tear of the medial meniscus, which is also well-visualized in the T2Sh image reformatted into coronal T2. Figure 4 presents a case of a 10-year-old female patient evaluated for ACL tear vs. avulsion following a ski accident. T2Sh images of the patient show a partial tear of the deep fibers of the medial collateral ligament with some mild associated subcortical edema. An avulsion injury from the tibial spine at the ACL attachment is also seen on the T2Sh images reformatted to coronal intermediate weighting and sagittal T2 weighting.

Figure 5 shows a 14-year-old male patient evaluated for internal derangement of the right knee following a soccer injury. The T2Sh image reformatted into axial PD is annotated to demarcate the patellar tendon, ACL fibers, meniscus, and medial collateral ligament (MCL). Coronal T2Sh images with intermediate weighting and T2 weighting show bone bruise and partial tearing/sprain of the MCL. The edema in the bone is well-visualized in the T2Sh sagittal source images, with contrast varying from PD to T2 weighting.

Figure 6 shows histograms and cumulative distributions of the number of days between exam order to exam registration for both the targeted knee MRI exam and the conventional knee MRI exam. Of the 49 targeted knee MRI orders, 20 exams (41%) were completed on the same day as requested. The median time from order to completion was 6 days (minimum of 0 days, maximum of 54 days). The cumulative distribution for the targeted knee MRIs shows that the majority of cases were completed in less than one week, and only a small number of cases took more than two weeks to complete. In comparison, no conventional knee MRI cases were completed on the same day as the order. The median time from order to completion was longer than that of the targeted knee exam (8 days), and a number of cases required multiple weeks to months of turnaround time. The time from order to completion for the targeted exam was significantly lower compared to the conventional exam (Wilcoxon rank-sum test, $p < .01$).

The histograms and cumulative distributions of exam times for both the targeted knee MRI and the conventional knee MRI are shown in Figure 7. Median time from registration to exam completion for the targeted MRI exam was 18:44 minutes (minimum of 10:28 minutes, maximum of 37:14 minutes). Mean and median exam times are similar, indicating few outliers. There were a large number of exams that took under 15 minutes to complete. This corresponds to 20 cases (41%) that did not have additional or repeated image sequences. Nonetheless, a number of cases had repeated scans, most often due to motion artifacts. There were 13 cases in which the 2D coronal T1 scan was repeated, and there were five cases in which the T2Sh scan was repeated. Additionally, seven cases included a 2D sagittal T2 FS scan at the discretion of the technologist. Finally, one case included an

additional 5-minute T2Sh research scan to evaluate image quality with a reduced acquisition time. In comparison, the median exam time for the conventional exam was 31:40 minutes (minimum of 23:49 minutes, maximum of 46:16 minutes). The targeted knee MRI reduced exam time on average by 40%. The exam times for the targeted exam were significantly lower compared to the conventional exam (Wilcoxon rank-sum test, $p < .01$).

Figure 8 shows three examples of failures in the T2Sh scan that required repeated or alternate scans. The first case shows artifacts due to patient motion during the scan, rendering the T2Sh and T1 coronal images non-diagnostic. The scans were subsequently repeated. The second example shows an instance where the non-imaged knee wrapped into the FOV due to the non-selective RF excitation and technologist error in patient positioning. The scan was repeated with the alternate leg placed farther from the imaging FOV. In the last case, the fat suppression failed, and the patient was moved to an alternate scanner. Taking into account this case, no patient had to return for additional imaging.

Figure 9 shows the histograms of the T2Sh processing times before and after the introduction of the distributed reconstruction. The median processing time before using the multi-node cluster was 18:48 minutes (minimum of 15:06 minutes, maximum of 83:35 minutes). There were two instances where the processing time exceeded 26 minutes. This was a result of using an older backup machine for the reconstruction while the load balance was not ideal on the hospital's computing resources. After deploying the distributed reconstruction, the median processing time[2,3] was reduced to 1:35 minutes (minimum of 1:09 minutes, maximum of 3:00 minutes). The dramatic speedup in processing times was primarily due to (i) the use of multiple machines for each reconstruction, and (ii) optimizing core components of the iterative reconstruction algorithm (20).

DISCUSSION

Accelerated scanning methods aim to reduce exam times and increase patient throughput in a clinical environment. An important component to the MR value equation is the cost to the patient. This study evaluated a targeted knee MRI exam that was designed for specific clinical indications in a pediatric population with the goal of reducing time, charges, and burden to the patient and family. The exam was based on T2Sh as a mechanism for obtaining fat-suppressed images in multiple orientations and contrasts. The T2Sh scan was paired with a 2D T1 coronal scan without fat suppression in order to obtain complementary information about bone marrow and anatomy. As the imaging time was reduced compared to the conventional knee MRI, a reduced charge CPT modifier code was used for insurance billing, lowering the technical fees to one third of the conventional knee MRI fee. Although the scan time reduction was less than one third, the cost of the targeted exam was only professional

[2]Performance results are based on testing as of May 30, 2018, and may not reflect all publicly available security updates. See configuration disclosure for details. No product can be absolutely secure.

[3]Software and workloads used in performance tests may have been optimized for performance only on Intel microprocessors. Performance tests, such as image reconstruction time, are measured using specific computer systems, components, software, operations and functions. Any change to any of those factors may cause the results to vary. You should consult other information and performance tests to assist you in fully evaluating your contemplated purchases, including the performance of that product when combined with other products. For more complete information visit www.intel.com/benchmarks.

costs of the radiologist and minimal costs associated with reporting infrastructure. The magnet, technologists, and receptionists were already present.

The targeted knee MRI exam was designed to fit in between already scheduled patients during the day. The purpose for this decision was so that patients could be seen the same day as their initial visit to the orthopedist. In this study, 20 of the 49 cases were scanned on the same day. A number of situations likely arose in which (i) the staffing schedule still could not accommodate the MRI, or (ii) the patients and parents elected to return on a different day as a matter of convenience. Although there was no obvious pattern based on age or time of year, the exam registration time was a positive predictor for likelihood of same-day scan: 15 of the 18 cases with exam registration between 2 pm and 6 pm were same-day orders. Conversely, only 5 out of 31 cases were same-day orders outside this window. This may indicate that patients who are seen by an orthopedic surgeon in the morning are more likely to be subsequently scheduled for their MRI later that day. In comparison, our institution had no instances of same-day scheduling for routine knee MRI prior to the introduction of the targeted knee exam.

After the deployment of the distributed reconstruction, the reconstruction times for T2Sh no longer impacted the technologists' workflows, as the images were available on the scanner console before the coronal T1 scan finished. As a result, the technologist could immediately review the images for quality and initiate the multi-planar reformats. The distributed cluster used four high performance compute nodes, each with a cost of about $10,000. Although the high cost may pose a barrier to the widespread use of the proposed MRI exam, the amortized cost is expected to be low, as similar targeted MRI exams can be developed for other joints to leverage T2Sh and other high-computation MRI methods. The authors in (20) simulated a scenario where every clinical scan required specialized parallel imaging and compressed sensing reconstructions, finding that two compute clusters could fully serve the reconstruction needs of a large hospital.

A major challenge with pediatric imaging is patient cooperation during the exam. Although on average the targeted knee MRI reduced the exam time, a large number of cases still had additional scanning. Surprisingly, the 2D coronal scan was repeated more often than the T2Sh scan. This may be a result of the lower risk in re-acquiring a three-minute scan versus the longer seven-minute T2Sh scan. A number of cases used additional 2D imaging sequences following the targeted protocol, likely related to technologist familiarity. As a result, the total scan time was greater than 20 minutes in about half the cases. The need to repeat scans poses a risk in the "on-demand" scheduling model, but it is not unique to the targeted knee MRI exam. In particular, motion during scans is common with pediatric patients and best mitigated through proper patient preparation (28, 29). Ongoing technologist training may impact this as well. Although it is possible for attending radiologists to provide image quality feedback before the patient leaves the table, this is not common for non-contrast joint MRI. Therefore, there may be a change in technologists' workflows and training, e.g. to identify when the single-sequence scan needs to be repeated. Nonetheless, the mean exam times were still nearly two times lower compared to the conventional lower extremity knee MRI.

Volumetric knee MRI has long been described and compared against 2D imaging. However, true penetration of the technique into clinical practice has been hindered by residual image blurring, likely from T2 decay over the long echo trains required for the volumetric technique. T2Sh eliminates this source of blurring, and hence, this work reports volumetric proton-density and T2 weighted imaging actually supplanting 2D FSE scanning in clinical practice. As no patient had to return for additional imaging, we have shown feasibility of the technique. Further, the impact of implementation was not only enabling same-day MRI in our practice for enhanced patient access and convenience, but also to reduce charges by two-thirds. A similar model may be possible for other exams based on one or two volumetric scans (15, 16). We are evaluating the use of T2Sh for other musculoskeletal exams in our institution, including a 5-minute reduced TR acquisition.

A limitation of this study was that arthroscopic data was not available to corroborate the MRI findings, though the focus of this study was on scheduling feasibility. A second limitation was that there was little control over the interplay between the orthopedic surgeons, radiologists, technologists, and patients. Thus, although the study presented a compelling case for inclusion of a high-value MRI exam, the volatility of the hospital workflow reduced the ability to accurately attribute cause and effect for scan times and patient throughput. A third limitation was the relatively small number of participants. The targeted knee exam was intentionally limited to a small subset of clinical indications and insurance pre-authorizations during its initial implementation, but further evaluation is required. Finally, the study was biased by only including subjects who were eligible for the targeted knee protocol. It is possible that the patients who were sub-selected based on insurance authorization were better equipped to accommodate an MRI exam under short notice, and furthermore were more cooperative during the exam.

In conclusion, this study has shown that a targeted knee MRI exam based on T2 Shuffling has the potential to reduce exam times and costs to the patients in a pediatric population.

Acknowledgements:

None

Grant Support: We thank the following funding sources: National Institutes of Health (NIH) grants R01EB009690, P41RR09784; Sloan Research Fellowship; Bakar Fellowship; GE Healthcare (research support)

REFERENCES

1. Pai DR, Strouse PJ. MRI of the pediatric knee. AJR Am J Roentegnol 2011;196:1019–1027.
2. Centers for Disease Control and Prevention. Nonfatal sports- and recreation-related injuries treated in emergency departments--United States, July 2000-June 2001. MMWR Morb Mortal Wkly Rep 2002;51.
3. Sheu Y, Chen LH, Hedegaard H. Sports- and Recreation-related Injury Episodes in the United States, 2011–2014. Natl Health Stat Report 2016;99:1–12.
4. Gill KG, Nemeth BA, Davis KW. Magnetic resonance imaging of the pediatric knee. Magn Reson Imaging Clin N Am 2014;22:743–763. [PubMed: 25442031]
5. Laor T, Jaramillo D. Pediatric musculoskeletal MRI: basic principles to optimize success. Pediatr Radiol 2008;38:379–391. [PubMed: 18046547]

6. Strouse P, Koujok K. Magnetic resonance imaging of the pediatric knee. Top Magn Reson Imaging 2002;3:277–294.
7. Mugler JP. Optimized three-dimensional fast-spin-echo MRI. J Magn Reson Imaging 2014;39:745–767. [PubMed: 24399498]
8. Pruessmann KP, Weiger M, Scheidegger MB, Boesiger P. SENSE: sensitivity encoding for fast MRI. Magn Reson Med 1999;42:952–962. [PubMed: 10542355]
9. Griswold MA, Jakob PM, Heidemann RM, et al. Generalized autocalibrating partially parallel acquisitions (GRAPPA). Magn Reson Med 2002;47:1202–1210. [PubMed: 12111967]
10. Lustig M, Donoho D, Pauly JM. Sparse MRI: The application of compressed sensing for rapid MR imaging. Magn Reson Med 2007;58:1182–1195. [PubMed: 17969013]
11. Busse RF, Brau ACS, Vu A, et al. Effects of refocusing flip angle modulation and view ordering in 3D fast spin echo. Magn Reson Med 2008;60:640–649. [PubMed: 18727082]
12. Kijowski R, Rosas H, Samsonov A, King K, Peters R, Liu F. Knee imaging: Rapid three-dimensional fast spin-echo using compressed sensing. J Magn Reson Imaging 2017;45:1712–1722. [PubMed: 27726244]
13. Fritz J, Raithel E, Thawait GK, Gilson W, Papp DF. Six-Fold Acceleration of High-Spatial Resolution 3D SPACE MRI of the Knee Through Incoherent k-Space Undersampling and Iterative Reconstruction-First Experience. Invest Radiol 2016;51:400–409. [PubMed: 26685106]
14. Lee SH, Lee YH, Suh JS. "Accelerating knee MR imaging: Compressed sensing in isotropic three-dimensional fast spin-echo sequence. Magn Reson Imaging 2018;46:90–97. [PubMed: 29103976]
15. Fritz J, Ahlawat S, Fritz B, et al. 10-Min 3D Turbo Spin Echo MRI of the Knee in Children: Arthroscopy-Validated Accuracy for the Diagnosis of Internal Derangement. J Magn Reson Imaging 2018; in press. doi: 10.1002/jmri.26241.
16. Chaudhari AS, Black MS, Eijgenraam S, et al. Five-minute knee MRI for simultaneous morphometry and T2 relaxometry of cartilage and meniscus and for semiquantitative radiological assessment using double-echo in steady-state at 3T. J Magn Reson Imaging 2018;47:1328–1341. [PubMed: 29090500]
17. Tamir JI, Uecker M, Chen W, et al. T2 shuffling: Sharp, multicontrast, volumetric fast spin-echo imaging. Magn Reson Med 2016;77:180–195. [PubMed: 26786745]
18. Bao S, Tamir JI, Young JL, et al. Fast comprehensive single-sequence four-dimensional pediatric knee MRI with T2 shuffling. J Magn Reson Imaging 2016;45:1700–1711. [PubMed: 27726251]
19. Tamir JI, Uecker M, Vasanawala SS, Lustig M. T2 Shuffling with Partial Fourier Acquisition and Reconstruction. In: Proceedings of the ISMRM Scientific Workshop on Data Sampling and Image Reconstruction, Sedona, 2016.
20. Anderson MJ, Tamir JI, Turek J, et al. Clinically Deployed Distributed Magnetic Resonance Imaging Reconstruction: Application to Pediatric Knee Imaging. Arxiv 2018; preprint. doi: arXiv: 1809.04195v1.
21. Zhang T, Pauly JM, Vasanawala SS, Lustig M. Coil compression for accelerated imaging with Cartesian sampling. Magn Reson Med 2013;69:571–582. [PubMed: 22488589]
22. Uecker M, Lai P, Murphy MJ, et al. ESPIRiT-an eigenvalue approach to autocalibrating parallel MRI: Where SENSE meets GRAPPA. Magn Reson Med 2014;71:990–1001. [PubMed: 23649942]
23. Iyer SS, Ong F, Doneva M, Lustig M. SURE-based Automatic Parameter Selection For ESPIRiT Calibration. Arxiv 2018; preprint. doi: arXiv:1811.05672v1.
24. Beck A, Teboulle M. A Fast Iterative Shrinkage-Thresholding Algorithm for Linear Inverse Problems. SIAM J on Imag Sci 2009;2:183–202.
25. Uecker M, Tamir JI. BART: version 0.4.02, Zenodo 2017. doi: 10.5281/zenodo.1066014.
26. Uecker M, Ong F, Tamir JI, et al. Berkeley Advanced Reconstruction Toolbox. In: Proceedings of the 23rd Annual Meeting of ISMRM, Toronto, 2015 (abstract 2486).
27. Noll DC, Nishimura DG, Macovski A. Homodyne detection in magnetic resonance imaging. IEEE Trans Med Imaging 1991;10:154–163. [PubMed: 18222812]
28. Camilo J, Gee MS. Strategies to minimize sedation in pediatric body magnetic resonance imaging. Pediatr Radiol 2016;46:916–927. [PubMed: 27229508]

29. Olsen ØE. MRI: how to perform a pediatric scan. Acta Radiologica 2013;54:991–997. [PubMed: 23390159]

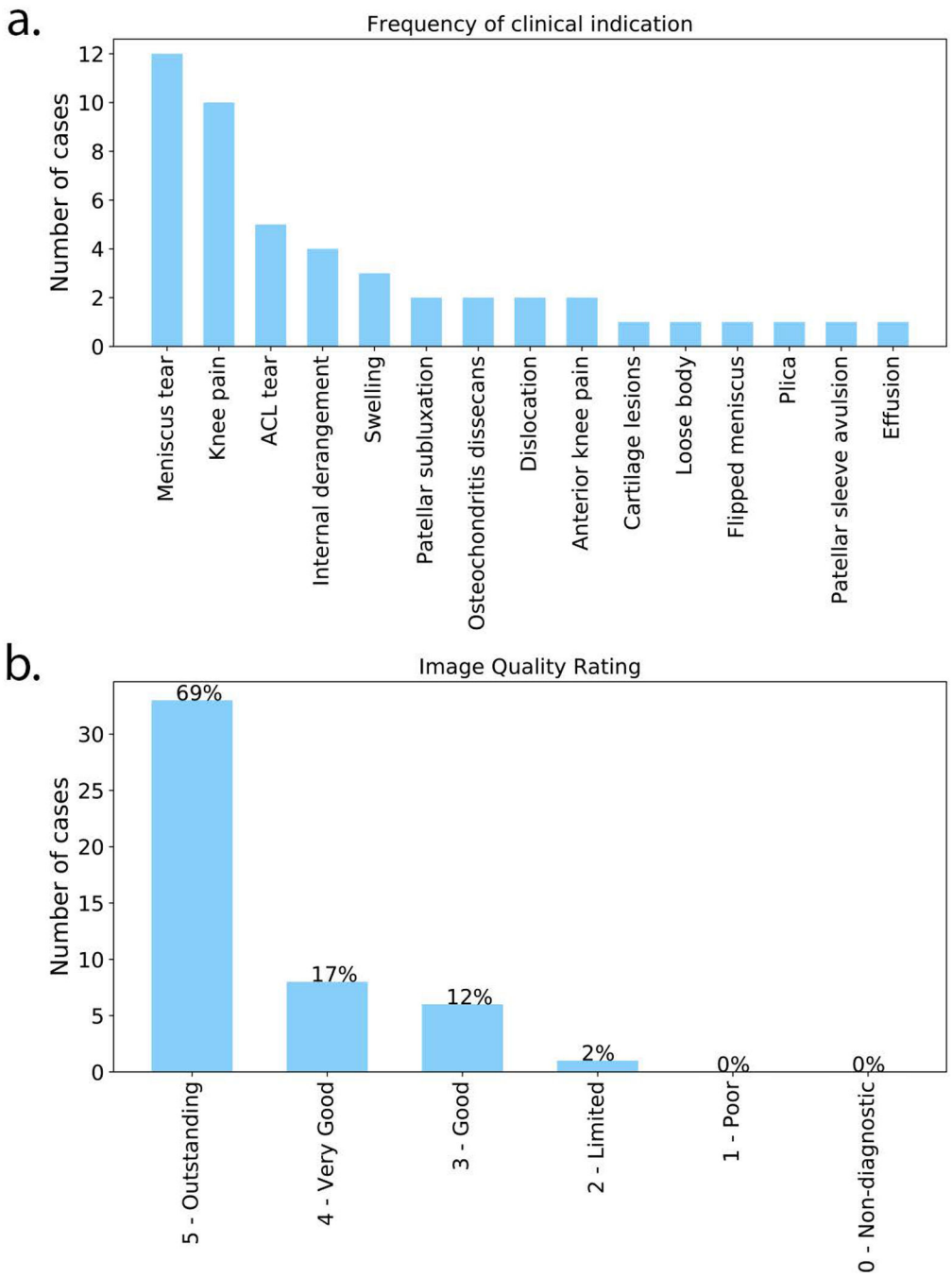

Figure 1.

(a) Bar chart of the primary clinical indication for each exam order. (b) Image quality assessment ratings after consensus was reached by two radiologists.

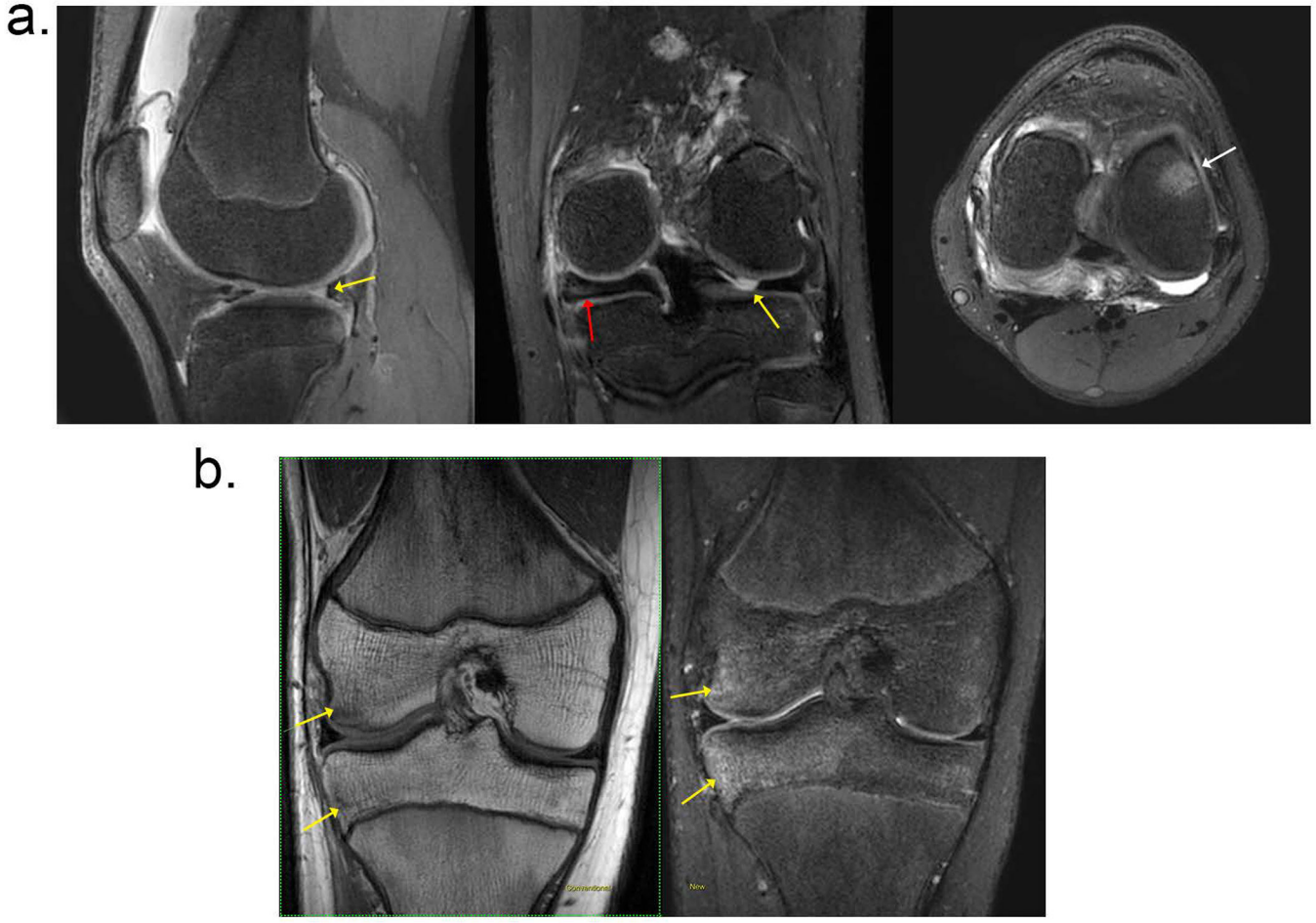

Figure 2.

Two patients with clinical indication of meniscal tear. (a) A 13-year-old female patient evaluated for internal derangement of the left knee. T2Sh images reformatted into (left) sagittal PD, (middle) coronal T2, and (right) axial intermediate weighting. Clinical suspicion of lateral meniscal tear was confirmed with MRI (yellow arrows). Additional related findings were medial discoid meniscus (red arrow) and bone marrow edema (white arrow). (b) Patient presented with knee pain and clinical suspicion of meniscal tear; (left) coronal nonfat-suppressed T1, and (right) T2Sh reformatted to coronal T2 weighted images are shown. Note the bone bruise, marked by the yellow arrows.

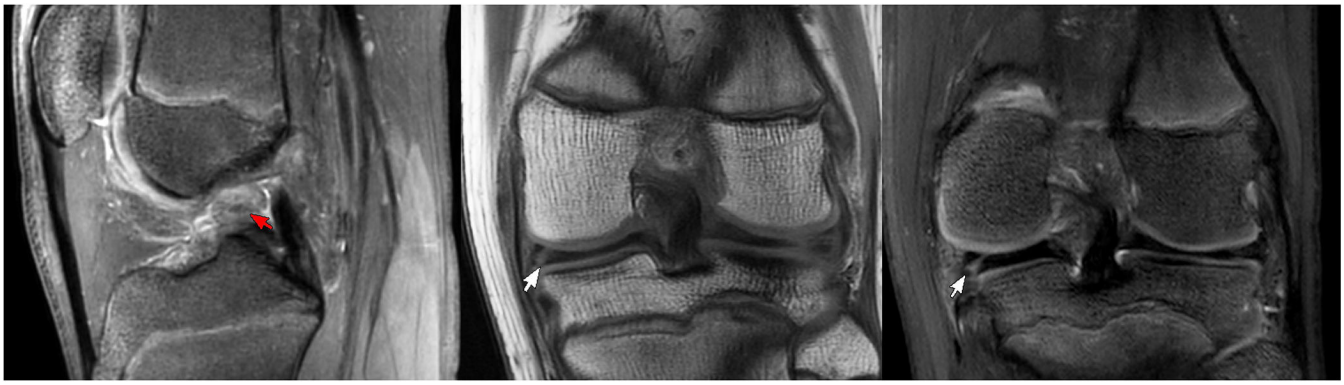

Figure 3.

A 15-year-old male patient evaluated for ACL/meniscus. T2Sh image reformatted into sagittal PD (left) shows high signal wavy ACL fibers consistent with high grade tear (red arrow). Coronal T1 (middle) and T2Sh image reformatted into coronal T2 (right) show tear of medial meniscus (white arrows).

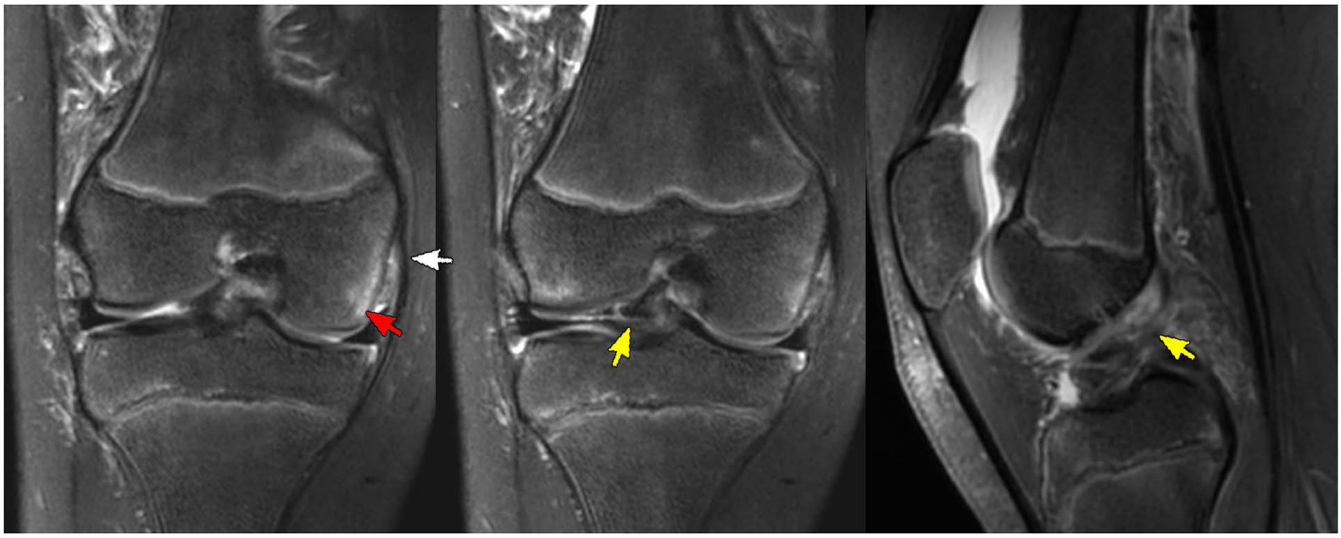

Figure 4.

A 10-year-old female patient with concern for ACL tear vs. avulsion with history of ski accident. Left: a partial tear of the deep fibers of the medial collateral ligament (white arrow) with some mild associated subcortical edema (red arrow) shown in the T2Sh image reformatted to T2 coronal. Avulsion injury from the tibial spine at the ACL attachment seen on T2Sh images reformatted to (middle) intermediate weighting coronal and (right) T2 sagittal planes (yellow arrows).

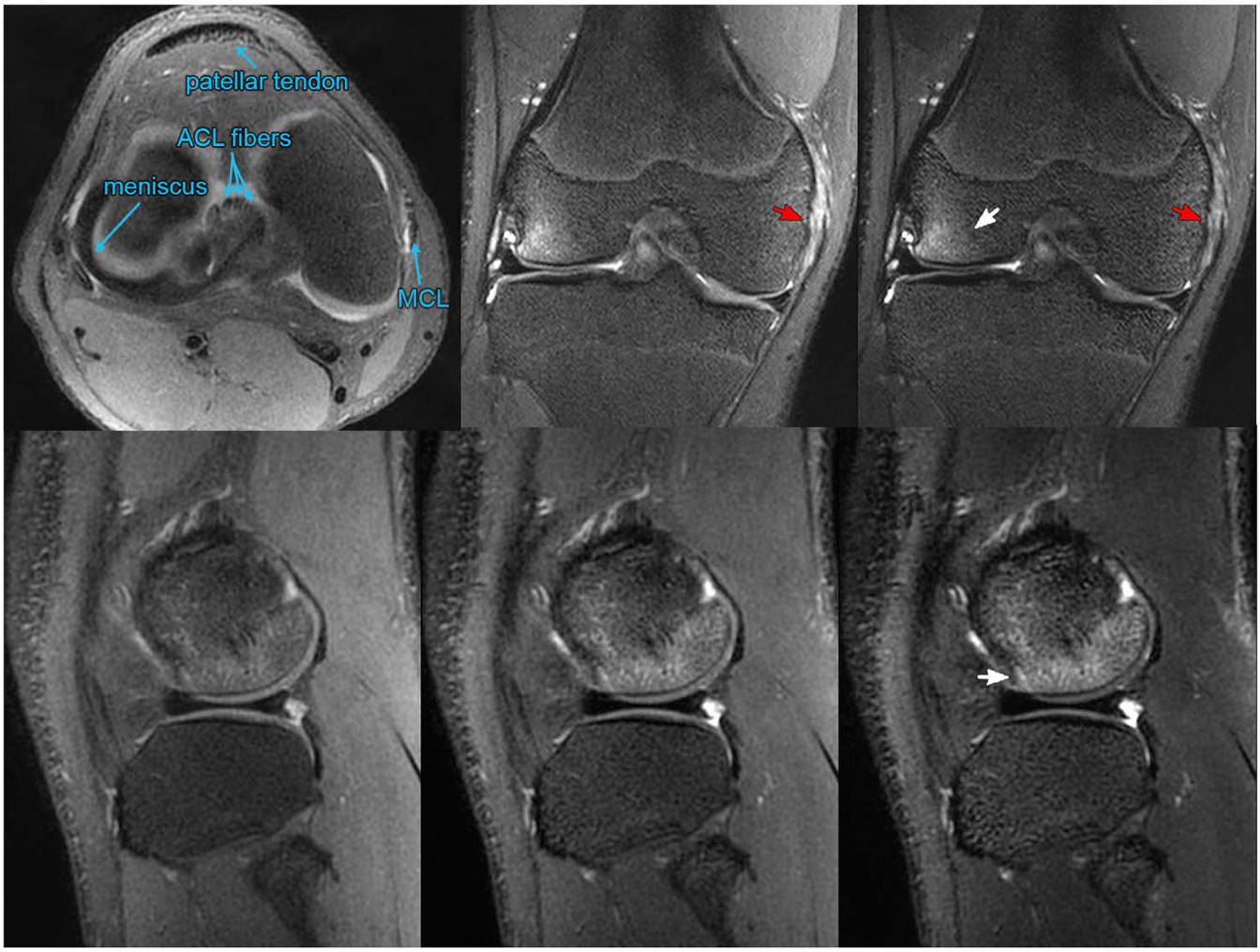

Figure 5.

A 14-year-old male evaluated for internal derangement of the right knee. Top left: annotated T2Sh image reformatted axially with PD contrast. The T2Sh images reformatted into intermediate and T2 weighted coronal planes (top middle and top right, respectively) show bone bruise (white arrow) and partial tearing/sprain of the medial collateral ligament (red arrows). T2Sh sagittal source images with (bottom left) PD, (bottom middle) intermediate weighting, and (bottom right) T2 weighting show the bone bruise (white arrow).

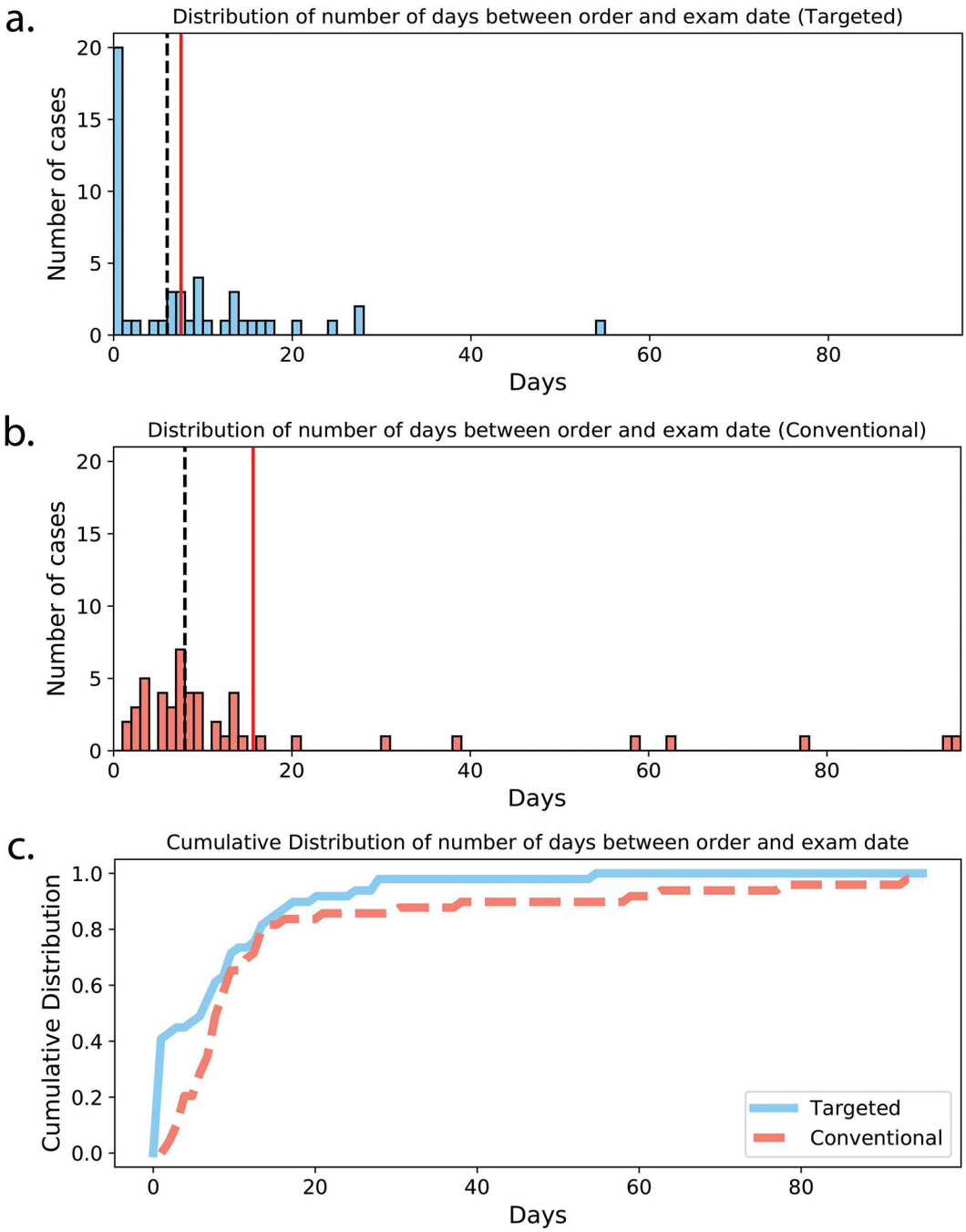

Figure 6.

Histograms of number of days between exam order and exam completion for (a) targeted knee MRI exam and (b) conventional knee MRI exam. Mean and median number of days are shown with solid red and dashed black lines, respectively. (c) Cumulative distributions for targeted (solid blue line) and conventional (dashed red line) order days.

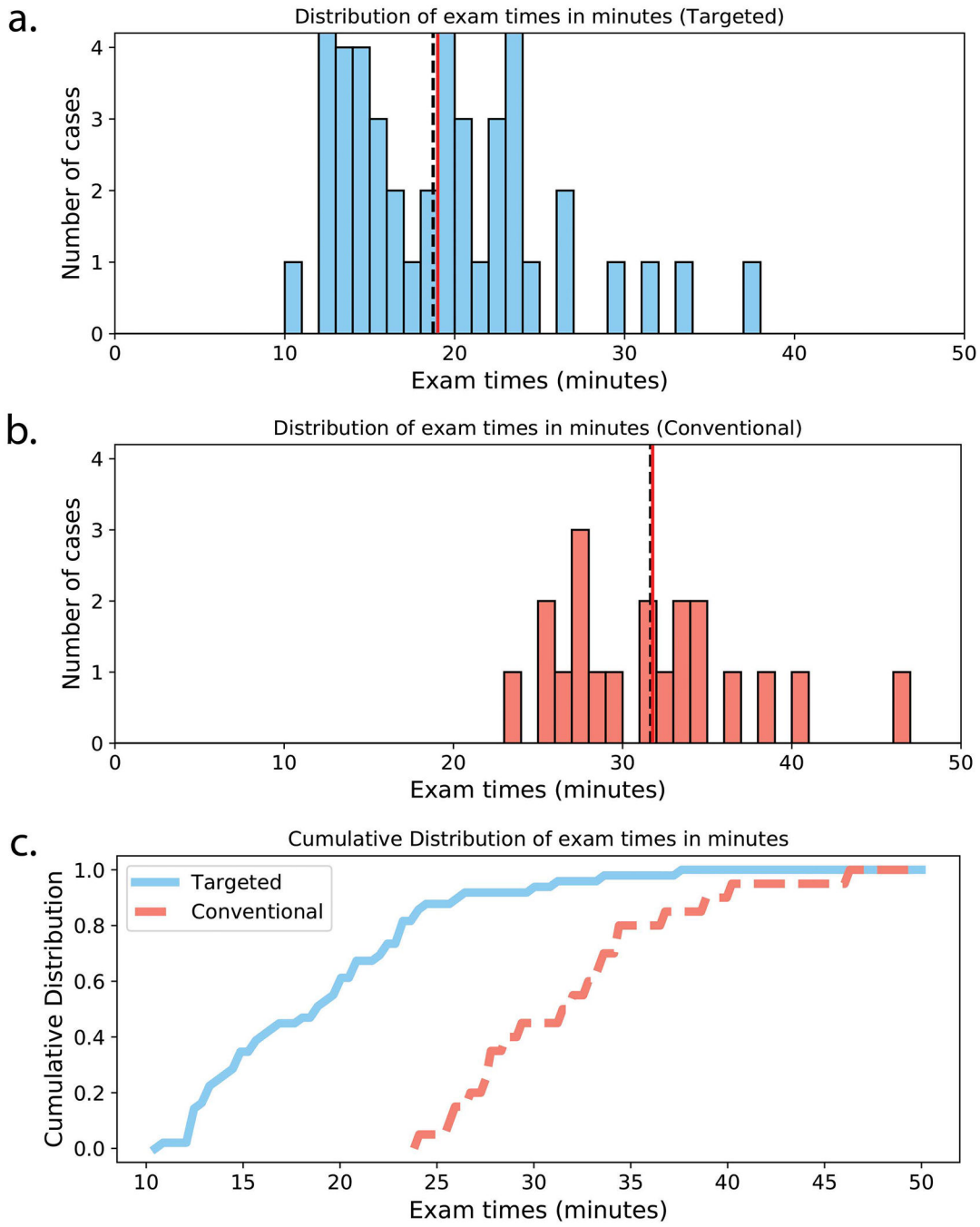

Figure 7.

Histograms of exam times for (a) targeted knee MRI exam and (b) conventional knee MRI exam. Mean and median exam times are shown with solid red and dashed black lines, respectively. (c) Cumulative distributions for targeted (solid blue line) and conventional (dashed red line) exam times.

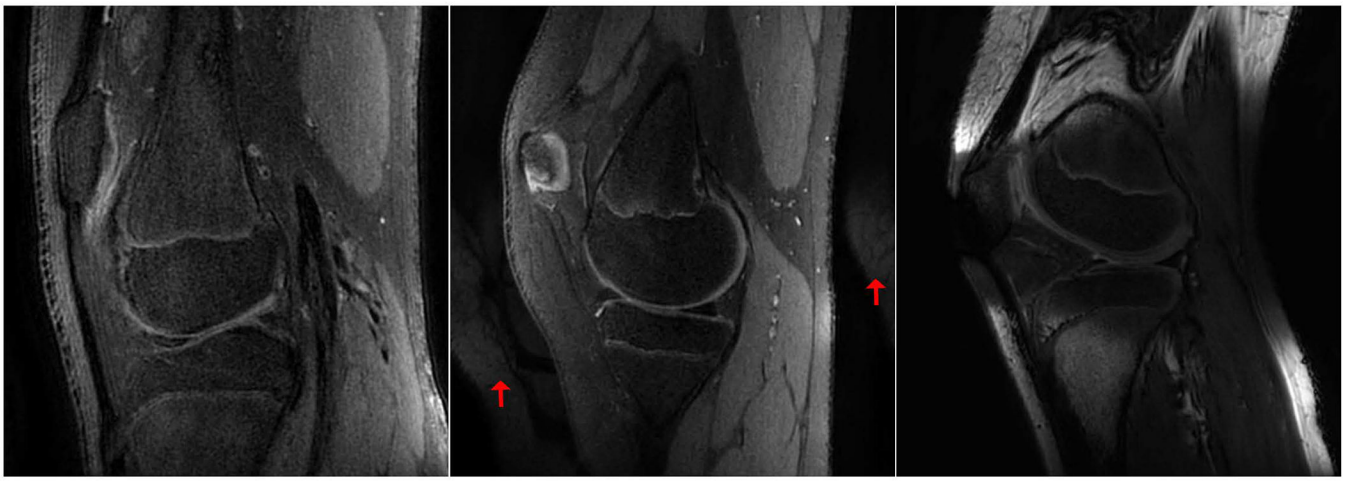

Figure 8.
Examples of T2Sh scans with suboptimal image quality. Left: motion during the scan reduced the apparent resolution. Middle: aliasing from other knee due to patient placement and a non-selective RF excitation (red arrows). Right: fat suppression failure during the scan.

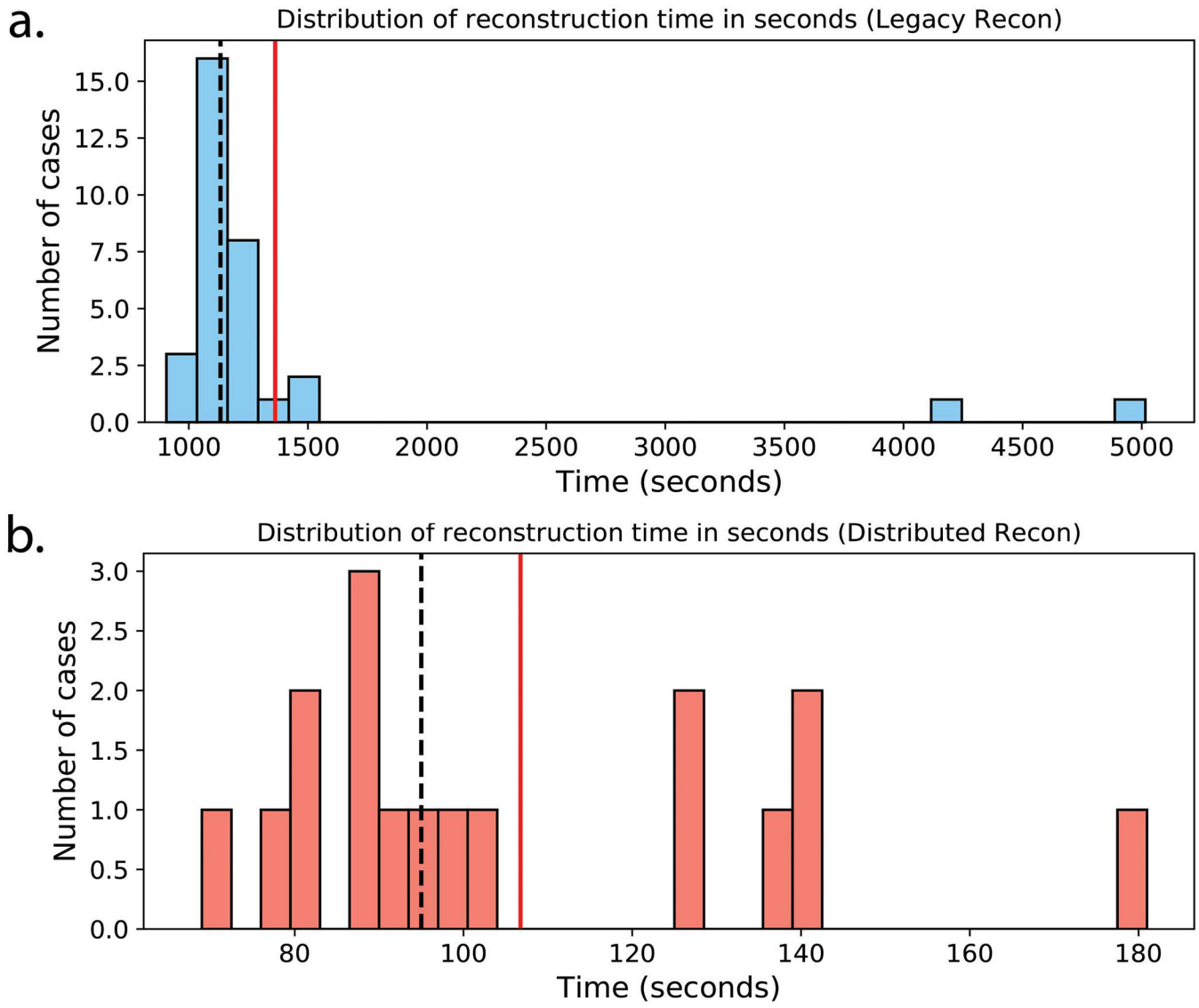

Figure 9.

Histograms of T2Sh reconstruction times in seconds (a) before and (b) after deployment of the optimized reconstruction with distributed processing. Note that the plot scaling differs due to the disparity in reconstruction times. Mean and median reconstruction times are shown with solid red and dashed black lines, respectively.

Table 1.

Targeted knee MRI typical scan parameters.

	3D Sagittal T2Sh FS	2D Coronal T1
TR (msec)	1200	700
TE (msec)	-	18
Echo spacing (msec)	6	8
Echo train length	83	3
Bandwidth (kHz)	62.5	50
Fat Saturation Efficiency	0.85	-
Field of view (cm^2)	16 × 14.4	14 × 12.6
Matrix size	288 × 260	416 × 288
Resolution (mm^2)	0.6 × 0.6	0.3 × 0.4
Slices	240	28
Slice thickness (mm)	0.6	2.5
Slice gap (mm)	-	0.5
Partial Fourier fraction	0.65	-
Scan time (min:sec)	7:04	2:50